URTeC: 5194

NMR Quantification of Wettability and Water Uptake in Unconventionals

M.J. Dick[1], D. Veselinovic[1], R. J. M. Bonnie[2] and S. Kelly[2]
[1]*Green Imaging Technologies, Fredericton, NB, Canada*
[2]*ConocoPhillips, Houston, TX*

Abstract

Consistent quantitative assessment of matrix wettability in tight rocks is critical for improved oil recovery (IOR) injection strategies. We applied a 3D SPRITE NMR pulse sequence to image spontaneous brine imbibition within an unconventional resource (UR) siltstone sample fully saturated with decane. To distinguish between brine and decane in the images and confirm oil saturations during the imbibition process, we used brine made with heavy water (D_2O), which is invisible to the NMR spectrometer. We previously presented a new diagnostic SCAL method for monitoring wettability changes in UR samples using a T_2-based NMR wettability index (NWI) measurement. Using that method, we monitored wettability changes over time for twin unconventional core samples undergoing oil-displacing-water and water-displacing-oil imbibition. In the current work, we advance validation of the budding UR NWI method by employing the aforementioned 3D NMR imaging techniques to visualize fluid front penetration within a sample as a function of time in 3D; i.e. yielding time-lapse or 4D water uptake data. These experiments reveal the distribution of the imbibing fluid, including if it completely penetrates the sample. Indeed, the time-lapse 3D NMR images of spontaneous uptake of water within a decane-saturated UR siltstone featured in this manuscript show that water fully penetrates the samples radially and that the process takes about two weeks to reach steady state. That stabilization time period is consistent with our previous bulk measurements results. This visualization work further validates our time-lapse NWI methodology for utilization in unconventionals. The multi-part UR NWI study yields a robust, repeatable, quantitative method for determining sample wettability and water uptake capacity which can be employed as an integration point for petrophysics, geology, geochemistry, and reservoir engineering and can help guide asset team completions fluid decisions.

Introduction

The work presented in this paper is a continuation of the work we completed previously [Kelly, S. et al., Kelly, S. et al.] on applying T_2-based NMR wettability index (NWI) measurement to unconventional samples to provide a robust wettability measurement for tight rocks. Specifically, our past results involved monitoring the change in wettability as function of time as saturated unconventional samples imbibed

decane or brine. These previous results involved measuring the bulk T_2 distributions of one sample in various sample states and then applying the NMR wettability analysis developed by Looyestijn [Looyestijn, W.J. et al., Looyestijn, W.J. et al.] to derive NWI. Briefly, to derive an NWI, NMR T_2 spectra of (1) 100% brine saturated sample, (2) 100% oil (decane) saturated sample, (3) bulk oil and (4) bulk brine are needed. These spectra are then mixed to give a predicted T_2 spectrum which is compared (via a least-squares fit) to a T_2 spectrum recorded from a sample partially saturated with both water and oil whose wettability is to be determined. In the past we have verified our results by determining the brine saturation independently by repeating the imbibition experiments with D_2O based brine in lieu of H_2O-based brine. D_2O is NMR invisible and as a result only signal from decane in the sample will be observed. This attribute allows the saturation of decane (and brine) to be calculated directly. The D_2O-based brine saturation can then be compared with the saturation derived from the NMR wettability analysis.

The previous results [Kelly, S. et al., Kelly, S. et al.] hinged on the assumptions that the samples are uniformly saturated and that the imbibed fluids fully penetrate the rock samples (cylindrical core plugs). Correspondingly, the bulk T_2 distributions measured and employed in NWI analysis are a true measure of the pore size distribution across the entire sample. This uniformity means the bulk T_2 distributions can be accurately employed to determine the NWI for the entire sample. In this paper, we set out to verify the assumptions that the samples are uniformly saturated and that imbibition is fully penetrating the core plugs radially by employing 3D NMR imaging techniques.

Theory and/or Methods

One of the twin siltstone samples studied in our previous work [Kelly, S. et al.] was selected for reanalysis with 3D NMR imaging techniques in this work; this sample's identifier is GP2. Figure 1 shows the results of the NMR wettability analysis previously reported [Kelly, S. et al.] for sample GP2. This sample was initially 100% decane saturated and spontaneously imbibed brine over time until steady state was reached. The wettability change for GP2 (Figure 1 – left panel – blue trace) shows that this sample started off oil wet and quickly became water wet (within a few days after submersion in water). The wettability predicted from the NMR analysis eventually stabilized between 0.2 and 0.4, indicating that the final wetting condition for the sample was mixed to slightly water wet. The brine saturation predicted from the NMR wettability analysis for twin GP2 (Figure 1 – right panel – blue trace) showed some oscillations in the first fifteen days. These oscillations are attributed to active changes ongoing within the rock during the initial water uptake, leading to instability in the predictions. After fifteen to twenty days, the water saturation of sample GP2 stabilized and slowly increased from about 20% to 45% by day fifty.

As mentioned earlier, the predicted saturation from the wettability analysis were validated employing D_2O based brine in lieu of H_2O based brine. D_2O is "NMR invisible" and, as a result, only signal from decane in the samples was observed. This approach allowed the saturation of decane (and brine) to be calculated directly. This D_2O-based brine saturation can then be compared with the saturation derived from the NMR wettability analysis. Figure 2 shows a typical example of a T_2 spectrum recorded for the same rock with H_2O-based brine versus D_2O based brine. For sample GP2, the D_2O analysis proceeded as follows. The sample was initially 100% decane saturated and allowed to imbibe an H_2O based brine. The experiment was then repeated with the rock again fully saturated with decane (care was taken to ensure that respective re-saturated NMR porosities matched the initial experiments) but this time it is allowed to imbibe D_2O-based brine. Both the saturation predicted by the NMR wettability analysis (Figure 1 – right panel – blue trace) and that derived from the D_2O data (Figure 1 – right panel – black trace) increased slowly from 0%

to 45% by day 50 of the experiment. The brine saturation then remained nearly constant at 45% for the remainder of the experiment.

For the 3D NMR imaging analysis completed in this work, the GP2 sample was again pressure saturated with decane and then submerged in a bath of D_2O-based brine. As in our previous work, the T_2 distribution of this sample was recorded periodically as the sample imbibed the D_2O brine. The volumes retrieved from this data were then employed to calculate the change in saturation as a function of imbibition time. This data was a direct repeat of our previous experiments and acted as a further validation of our previous work as well as a display of the consistency of the sample's water uptake capacity following hydration-dehydration cycles associated with experiment sample preparation. In addition to the T_2 distribution data, 3D images of sample GP2 were also recorded periodically as D_2O brine imbibition occurred. As with the T_2 data, the 3D images only show signal from the decane within the rock. As such, changes in the intensity of pixels over time are a direct measure of the change in decane saturation over time. In other words, the uniformity or lack of uniformity of the imbibition of the D_2O into the rock can be directly measured via the 3D images.

The NMR T_2 spectra for the wettability analysis were acquired with a GeoSpec NMR spectrometer from Oxford Instruments [Geo-Spec 12-53 User Manual] operating at 12 MHz. Green Imaging Technologies software was employed for data acquisition and analysis [GIT Systems User Manual]. The T_2 spectra are measured using a Carr-Purcell-Meibloom-Gill NMR pulse sequence [Meiboom, S. and Gill, D.] and Table 1 summarizes the NMR parameters employed for this sequence. The 3D images were recorded by employing a SPRITE pulse sequence [Balcom, B.J.]. Table 2 summarizes the NMR parameters employed for these images. The image resolution of our data was approximately 2.2 mm.

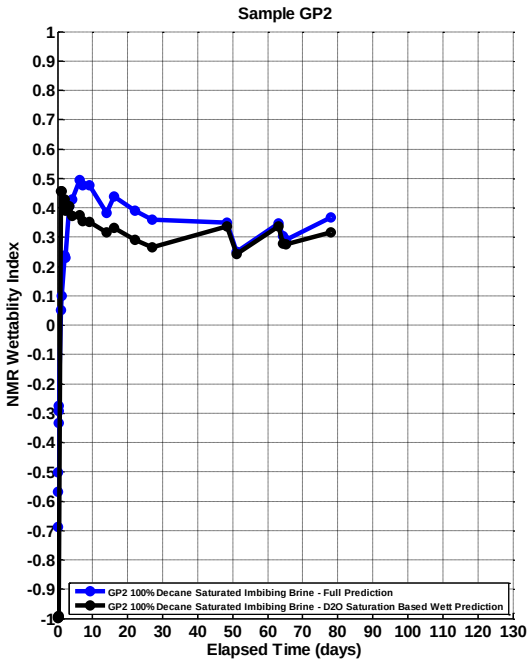

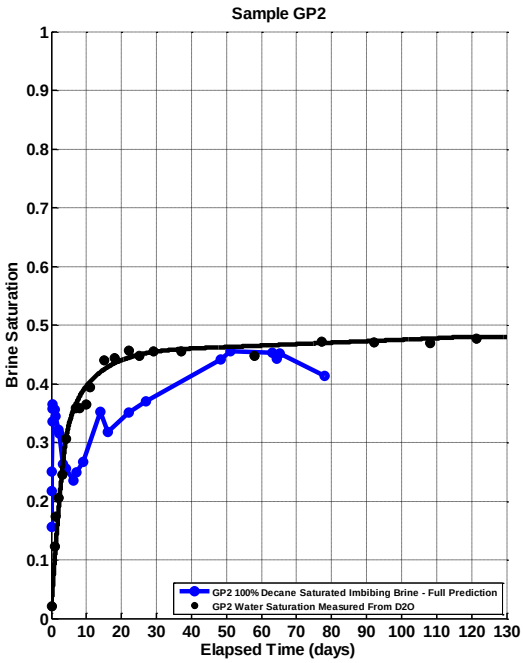

Figure 1: The results of the wettability analysis completed previously [Kelly S. et al.] for sample GP2 are shown. The left-hand panel shows the wettability index as a function of imbibition time for the sample, while the right-hand panel shows the water saturation as a function of imbibition time for the sample.

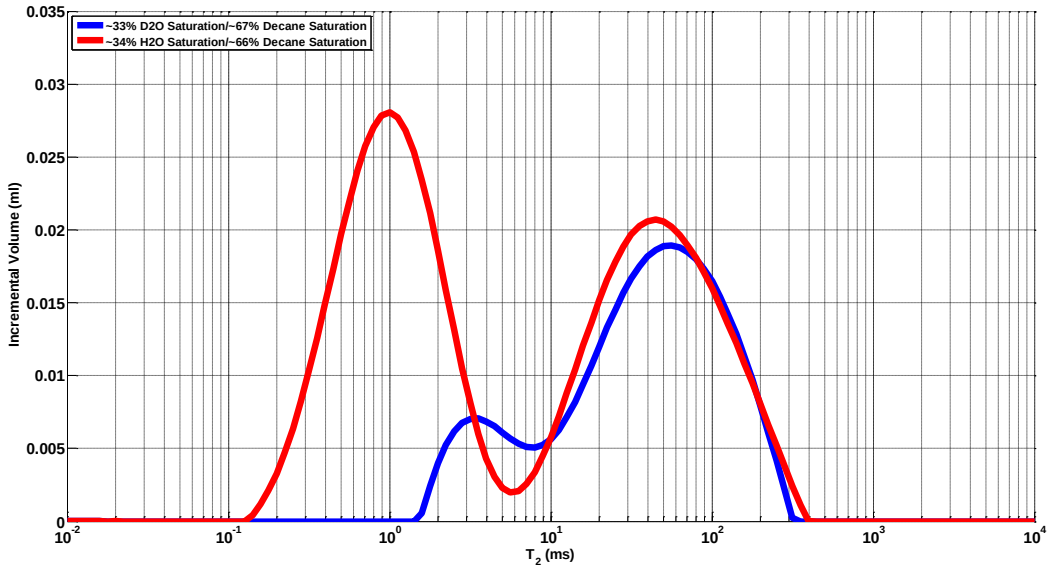

Figure 2: Typical example of T_2 pore size distributions measured with both D_2O (blue trace) and H_2O (red trace) based brines for the same rock at similar saturations. The peak at the lower T_2 values in the H_2O distribution is due to pores filled mostly with water while the peak at higher T_2 values is due to pores filled with decane. The distribution recorded with D_2O based brine only shows the signal from the decane so the second peak in the distribution is mostly visible. The first peak intensity has been greatly reduced because not much decane fills the smallest pores.

Table 1 – NMR CPMG Parameters

Pulse Sequence	Recycle delay (ms)	Signal to Noise Ratio	Tau (µs)	Number of Echoes	P90 (µs)
CPMG	750	200	50	5000	7.61

Table 2 – NMR 3D SPRITE Parameters

Pulse Sequence	Recycle delay (ms)	Signal to Noise Ratio	Flip Angle (deg)	Fraction of k-space encoded	Max. Gradient Strength (g/cm)
3D SPRITE	750	200	5	0.118	10.74

Results

Three dimensional images and T_2 distributions were recorded periodically for thirty days as sample GP2 imbibed D_2O brine. Initially, the data showed a good correspondence between the observed volume of decane derived from the T_2 distribution and the intensity of the 3D images both slowly decreasing.

Eventually, a large peak above 200 ms was observed in the T_2 distribution (Figure 3 – left hand panel). At that time, bubbles appeared on the surface of the sample in the 3D images (Figure 4 – left hand panel). It was initially hypothesized that the peak and bubbles were a result of decane being expelled from the sample as D_2O imbibed into the sample. To remove the signal from this large peak in the T_2 distributions a cut-off was applied to the data (Figure 3 – left hand panel – black dash). Any signal above 200 ms was not included in the analysis to determine the saturation of the sample. Figure 5 shows the brine saturation (brown trace) derived from the T_2 distribution data recorded for sample GP2. As can be seen from the figure, the latest data set agrees very well with the brine saturation measured previously using D_2O (Figure 5 - black trace). This result gave us further confidence that saturations derived from the D_2O data were accurate.

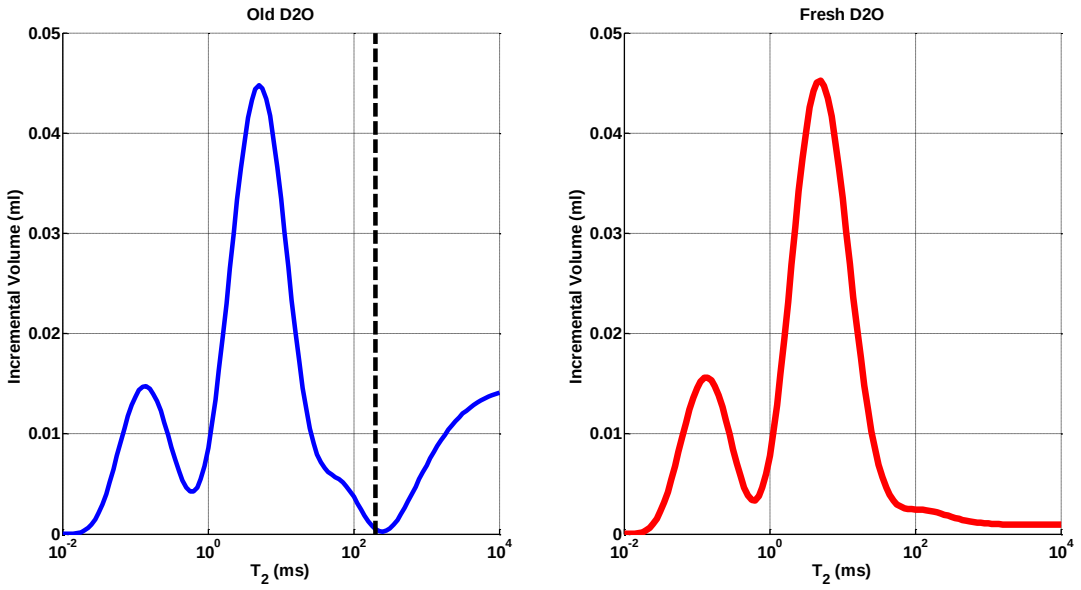

Figure 3: Bulk-T_2 spectra recorded as sample GP2 sat in a bath imbibing D_2O. The left-hand panel shows the original T_2 spectrum recorded in the original D_2O bath. The large peak above 200 ms is a result of hydrogen-deuterium oxide (HDO) present in the bath caused by H-D exchange between the D_2O and H_2O in the air. The right-hand panel shows the T_2-distribution recorded when the sample was placed in a bath of fresh D_2O. The large peak above 200 ms has been eliminated as the HDO has been removed.

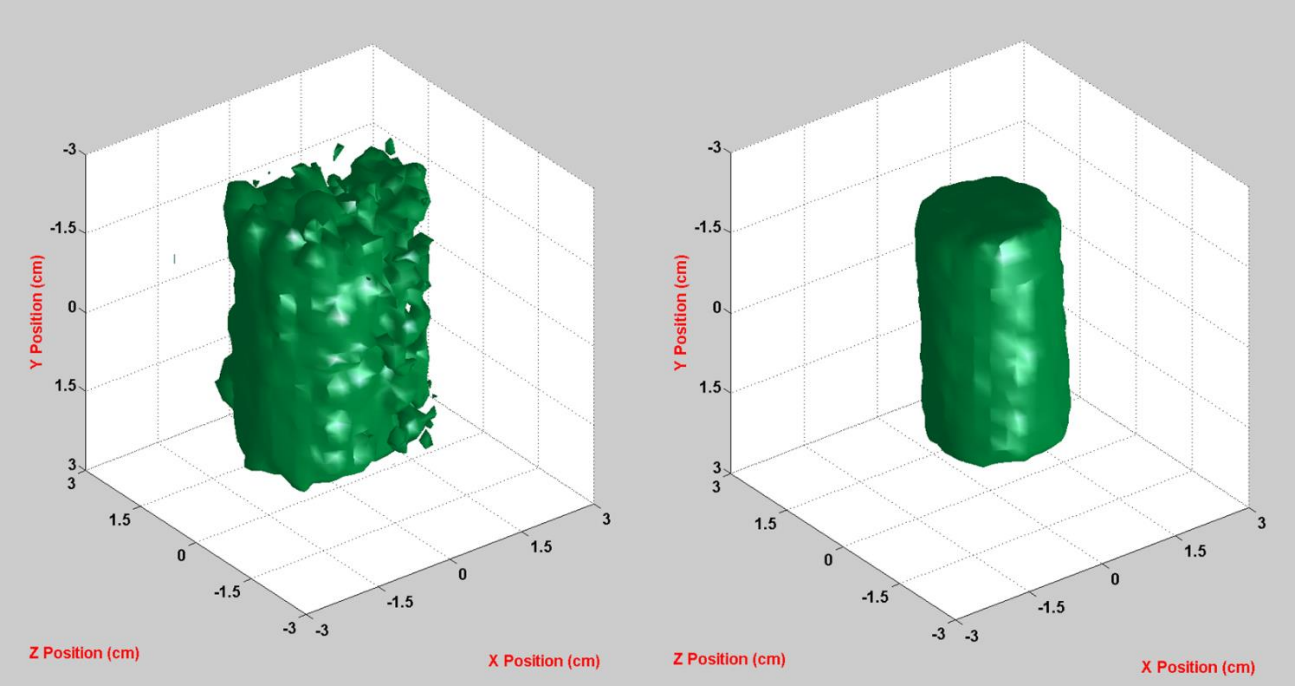

Figure 4: Three-dimensional images recorded as sample GP2 sat in a bath imbibing D_2O. The left-hand panel shows the original T_2 spectrum recorded in the original D_2O bath. The bubbles on the surface of the sample are a result of HDO present in the bath caused by H-D exchange between the D_2O and H_2O in the air. The right-hand panel shows the image recorded when the sample was placed in a bath of fresh D_2O. The bubbles were eliminated as the HDO was removed.

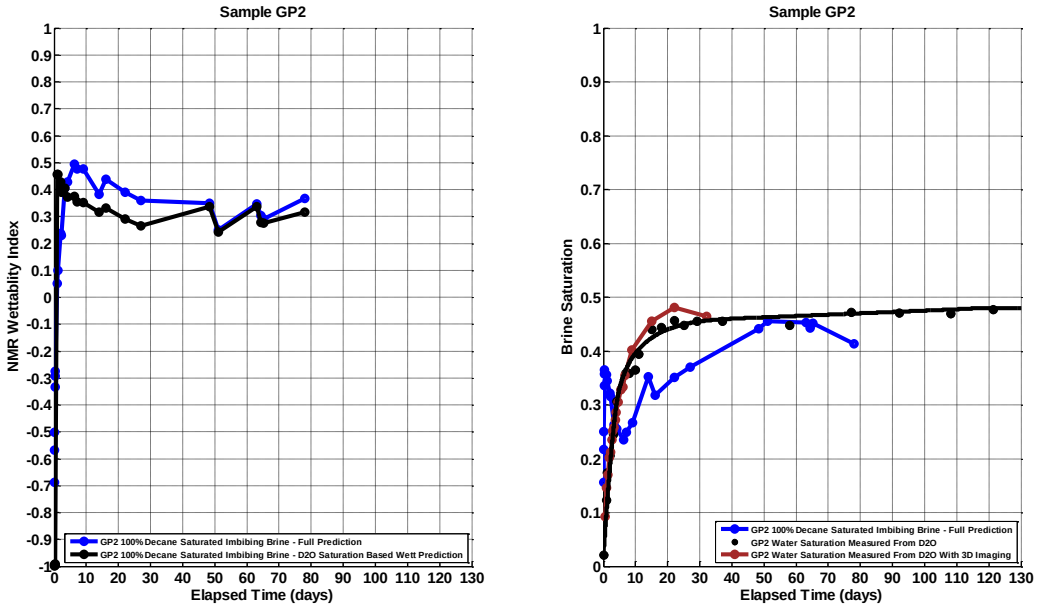

Figure 5: The results of the wettability analysis for sample GP2 are shown. The left-hand panel shows the wettability index as a function of imbibition time for the sample, while the right-hand panel shows the water saturation as a function of imbibition time for the sample. The brown trace is the water saturation vs time determined from the T_2-distribution data recorded in this study and is very well aligned with the previous data.

The primary purpose of the 3D data was to confirm whether the radial imbibition front penetrated the entire rock. To test this hypothesis, the three-dimensional image data was analyzed by summing the data from each pixel of the image along length of the sample (Y-axis) onto the XZ plane (Figure 6 – left most panel). Next, four regions of interest within this collapsed image were selected for study. As can be seen in the four right panels of Figure 6, these regions of interest were cylindrical each one getting successively further from the center of the plug. The average intensity per pixel within each of these regions of interest was then determined. It should also be noted that region 4 (Figure 6 – Lower right panel) was purposely chosen to not encompass the outer surface of the sample. This was so that none of the bubbles forming on the surface would be included in the intensity vs time analysis.

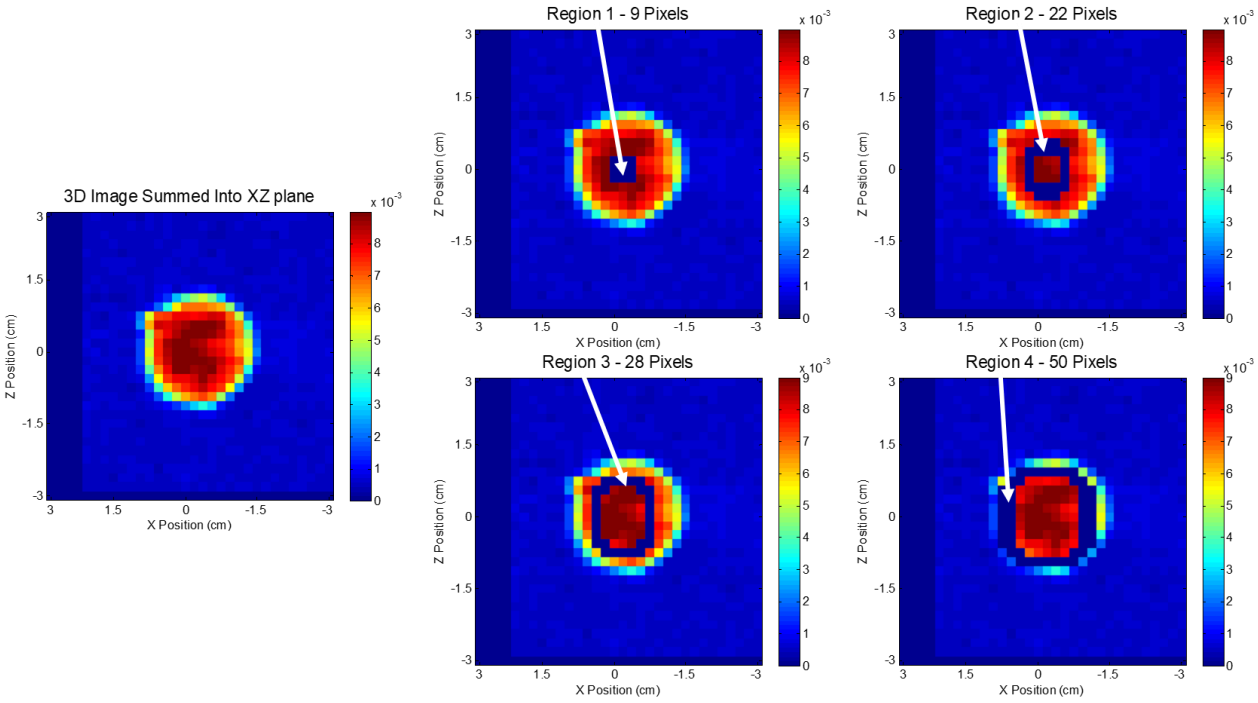

Figure 6: Left most panel shows the results of summing the three-dimensional image data for each pixel along length of the sample (Y-axis) onto the XZ plane. Four regions of interest within this collapsed image were selected for study (Right four panels). These regions of interest were cylindrical each one getting successively further from the center of the plug. The average intensity per pixel within each of these regions of interest (area highlighted in dark blue) was then determined.

Figure 7 shows the relative change in average intensity per pixel vs elapsed time for each of the four regions of interest shown in Figure 6. As expected, the average intensity per voxel drops over time for each region of interest. This is because D_2O is imbibing into the rock and displacing the decane. In addition, Figure 7 shows that the average intensity per pixel changes slower the further from the imbibition front the region of interest is. For example, the average intensity per pixel for region one (the inner most region of interest) takes about twenty days to decrease by 20%. Conversely, region four (the outer most region of interest) takes only about five days to decrease by 20%. However by day twenty, all regions of interest have seen their intensity drop by approximately 20%. This observation is consistent with the T_2 data (Figure 5 – right hand panel– brown and black traces) which shows that it takes about twenty days for the brine saturation in the rock to stabilize. This analysis also indicates that the D_2O is imbibing to the center of the sample.

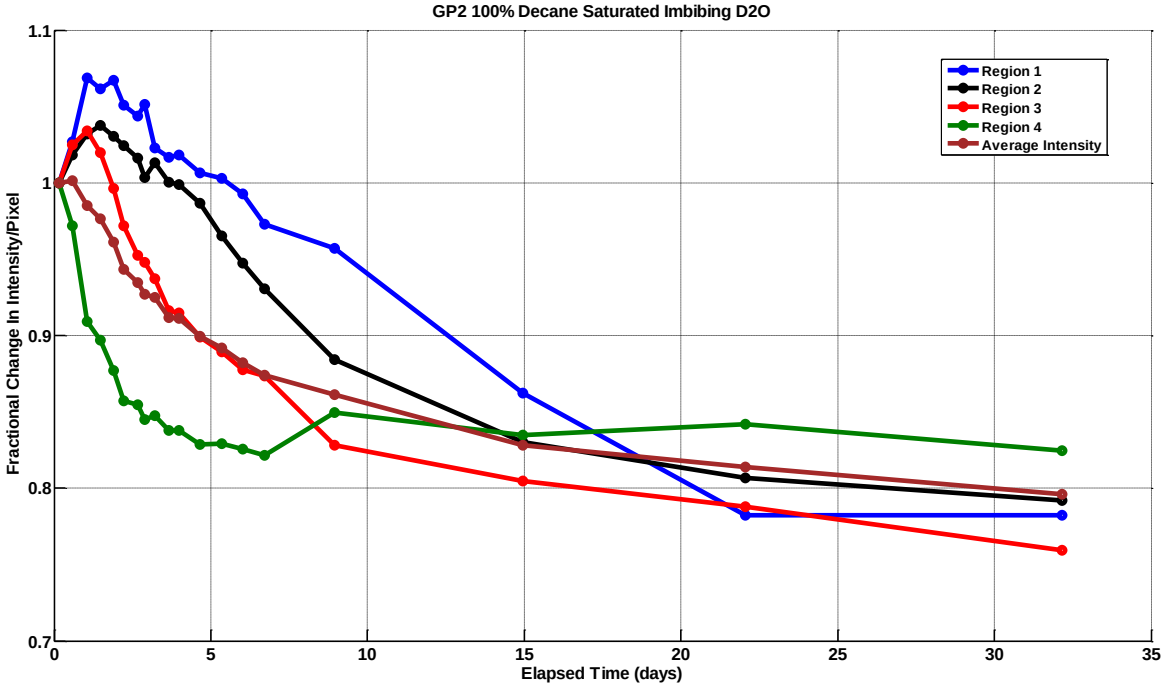

Figure 7: The relative change in average intensity per pixel vs elapsed time for each of the four regions of interest (Figure 6) is shown. As expected, the average intensity per pixel drops over time for each region of interest. This is because D_2O is imbibing into the rock and displacing the decane. In addition, the traces show that the average intensity per pixel changes slower the further from the imbibition front the region of interest is. The brown trace shows the relative change in intensity per pixel averaged across all regions of interest. Because the NMR signal is coming from only the decane present in the sample, this average intensity per pixel is proportional to the decane saturation for the entire sample.

Also shown on Figure 7 is the relative change in intensity per pixel averaged across all regions of interest (brown trace). Because the NMR signal is coming from only the decane present in the sample, this average intensity per pixel is proportional to the decane saturation for the entire sample. The intensity per pixel for the fully saturated rock is fixed to one. The brine saturation for the sample can then be calculated by subtracting the decane saturation from one. This calculated brine saturation can then be compared to the brine saturation measured previously for the sample via the T_2 distributions (Figure 5 – right hand panel– brown trace). Figure 8 shows that the brine saturation predicted from the average intensity per pixel data (purple trace) does not agree well with the brine saturation measured in this work via the T_2 distribution data (gray trace). Around day twenty, there is a nearly thirty percent disagreement in the brine saturation retrieved from the two methods (50% brine saturation from T_2 data vs. 20% brine saturation from average pixel data). This disagreement was of concern and led to further investigation of the data sets.

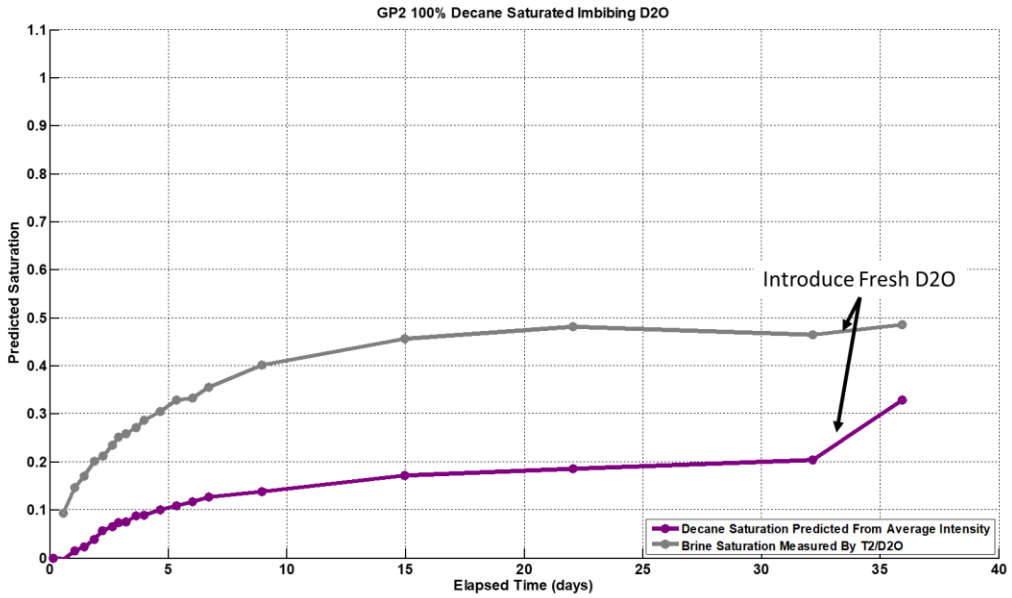

Figure 8: The brine saturation predicted by the average intensity per pixel from the three-dimensional image (purple trace) does not agree well with the brine saturation measured via the T_2 distribution data (gray trace). The last data point of the purple trace shows that the saturation derived from three-dimensional image data recorded after the sample was introduced into a fresh D_2O bath agreed better with the brine saturation derived T_2 distribution data.

Specifically, we took another look at the peak above the 200 ms cutoff in the T_2 distribution data (Figure 3 – left hand panel). As mentioned previously, this excess signal was attributed to decane being expelled from the sample as D_2O imbibed into the sample. This excess decane was also thought to be the source of the bubbles observed forming on the surface of the sample while it was submerged in the D_2O bath (Figure 4 – left hand panel). However, when more care was taken to fully characterize the peak above 200 ms, the volume of decane attributed to this peak was greater than the pore volume of the sample. Therefore, it was impossible for the observed excess signal to come solely from decane being expelled from the rock and there had to be another source of NMR signal in the D_2O bath. The most likely candidate was HDO formed within the bath via H-D exchange between the D_2O and water in the air. It should be noted that care was not taken to seal the D_2O bath from the air. In theory, signal from HDO should not have affected the results because for the T_2 distribution data a cutoff was applied to eliminate the HDO signal from the analysis and for the image data the HDO signal should have been outside the sample and outside the field of view of the magnet. However, in practice NMR signal from outside the field of view of the magnet can be inadvertently folded into the field of view of the magnet. This occurrence can lead to a higher-than-expected decane signal observed within the three-dimensional image of the rock leading to an underestimate of the amount of D_2O brine that has imbibed into the sample.

To test this hypothesis, the D_2O in the bath was replaced with fresh D_2O that had been sealed from exposure to air. New T_2 distributions and three-dimensional images were then recorded of sample GP2 in this bath. The right-hand panel of Figure 3 shows the T_2 distribution recorded with the fresh D_2O. Replacing the D_2O clearly eliminated the excess peak above 200 ms. This T_2 distribution data was then used to again calculate the brine saturation of the sample. The last data point of the gray trace in Figure 8 shows that the brine

saturation calculated with the fresh D_2O bath is consistent with the saturations derived previously with the HDO contaminated bath employing the 200 ms cutoff. This gave us confidence that the saturations derived from all the T_2 data were correct.

The right-hand panel of Figure 4 shows the three-dimensional image recorded after the D_2O in the original bath had been replaced with fresh D_2O and the sample surface was wiped with paper towel to remove any fluids on the surface. Clearly, replacing the D_2O eliminated any bubbles observed on the surface of the sample. This new three-dimensional image was then employed to determine the brine saturation via analysis of the relative change in intensity for each pixel within the image. The last data point of the purple trace in Figure 8 shows that the saturation derived from this new three-dimensional image data agreed better with the brine saturation derived D_2O T_2 distribution data. However, per this last data point, there was still an approximately 15% disagreement between the brine saturation derived from the two methods. This disagreement is most likely a result of HDO which had imbibed into the rock before the bath was revitalized with fresh D_2O. Signal from this excess HDO within the rock would be attributed to decane leading to an overestimate of the decane saturation within the sample and hence an underestimate of brine saturation within the sample.

To test this hypothesis, sample GP2 was dried, resaturated with decane and put into a new D_2O bath. This time care was taken to seal the D_2O bath from the surrounding air. Figure 9 shows the result of this resaturation test. The green trace in Figure 9 shows the brine saturation derived from the T_2 distribution data. It shows excellent agreement with the brine saturation data derived from the T_2 distribution data completed previously (Figure 9 – gray trace). This marks the third time this D_2O imbibition experiment was completed on sample GP2 and each time the results agreed well with one another as well as agreed with the brine saturation predicted from the original wettability analysis (Figure 5 – right hand panel – blue trace). The brine saturation derived from the three-dimensional data for this latest D_2O imbibition data is plotted in blue in Figure 9. For the first fifteen days, the agreement between the brine saturation predicted from the three-dimensional data and that derived from the T_2 distribution data was not perfect. However, the agreement was closer than it had been in the first iteration of this D_2O imbibition experiment (Figure 9 – purple vs. gray traces). Clearly, the parafilm seal employed on top of the NMR tube containing the GP2 sample and the D_2O bath in this iteration of the test along with periodically introducing fresh D_2O to the system helped reduce the presence of HDO. In the first iteration of the test, no seal was employed on top of the NMR tube and fresh D_2O was only introduced prior to the last data point. However, because the agreement between the T_2 and three-dimensional saturations was not perfect a further change was made to the system following the introduction of fresh D_2O on day sixteen. The parafilm seal was replaced with a rubber stopper in the hopes that the stopper would better seal the D_2O in the tube from exposure to water in the air. Following the introduction of the rubber stopper, the brine saturation predicted from the three-dimensional data (Figure 9 – blue trace) began to agree perfectly with the saturation derived from the T_2 distribution data (Figure 9 – green trace). This result gave concrete proof that the disagreement between the brine saturation derived from the T_2 data and that derived from the three-dimensional data was a result of the presence of HDO in the system. Now that it has been eliminated, our three-dimensional data is valid and truly reflecting what is occurring within the core sample.

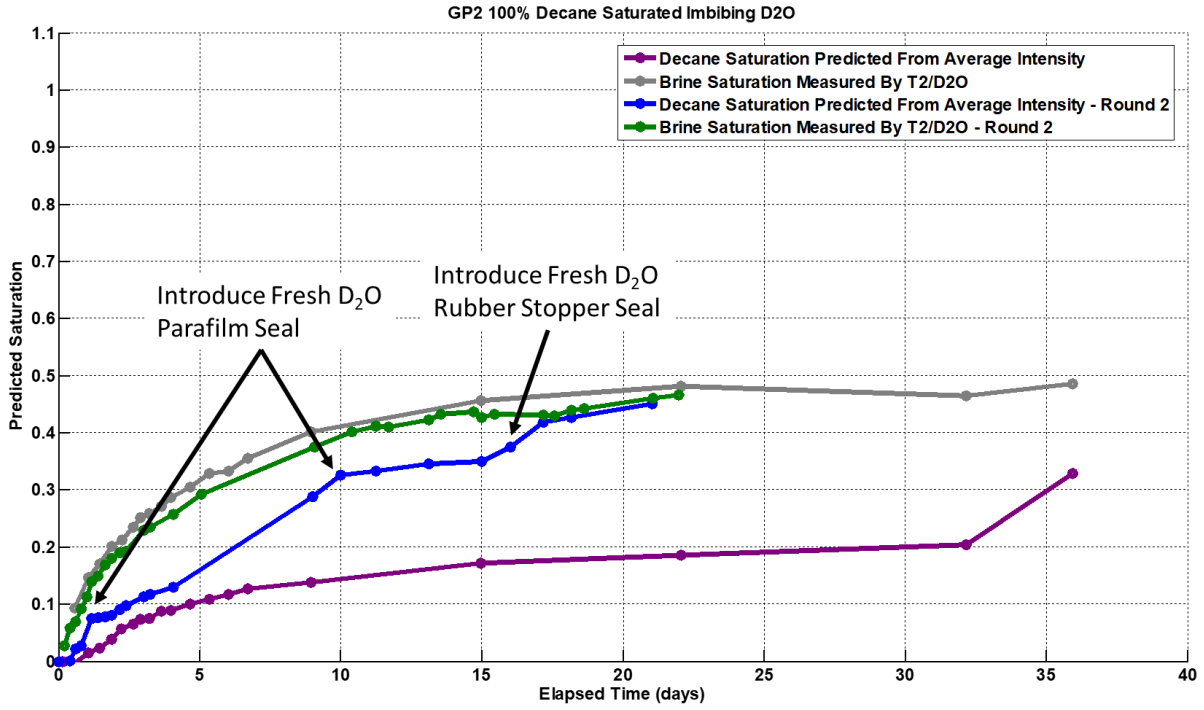

Figure 9: The D_2O imbibition experiment was repeated this time taking care to seal the D_2O bath. The green trace shows the brine saturation derived from the T_2 distribution data. It shows excellent agreement with the brine saturation data derived from the T_2 distribution data completed previously (gray trace). The brine saturation derived from the three-dimensional data for this latest D_2O imbibition data is plotted in blue. For the first fifteen days, the agreement between the brine saturation predicted from the three-dimensional data and that derived from the T_2 distribution data was not perfect. However, the agreement was closer than it had been in the first iteration of this D_2O imbibition experiment (purple vs. gray traces). The agreement improved following day sixteen, when the original parafilm seal was replaced with a rubber stopper. The brine saturation predicted from the three-dimensional data (blue trace) began to agree perfectly with the saturation derived from the T_2 distribution data (green trace).

Figure 10 shows the relative change in average intensity per pixel vs elapsed time for each of the four regions of interest shown in Figure 6. As with the previous iteration of this D_2O imbibition experiment (Figure 7), the average intensity per voxel drops over time for each region of interest. This is because D_2O is imbibing into the rock and displacing the decane. The data plotted in Figure 10 again shows that the average intensity per pixel changes slower the further from the imbibition front the region of interest is. For example, the average intensity per pixel for region one (the inner most region of interest) takes about twenty-five days to decrease by 25%. Conversely, region four (the outer most region of interest) takes only about nine days to decrease by 25%. However, by day twenty, all regions of interest have seen their intensity drop by about 40%. This observation is consistent with the previous three-dimensional data (Figure 7) and confirms that the imbibition front takes about three weeks to fully penetrate the sample.

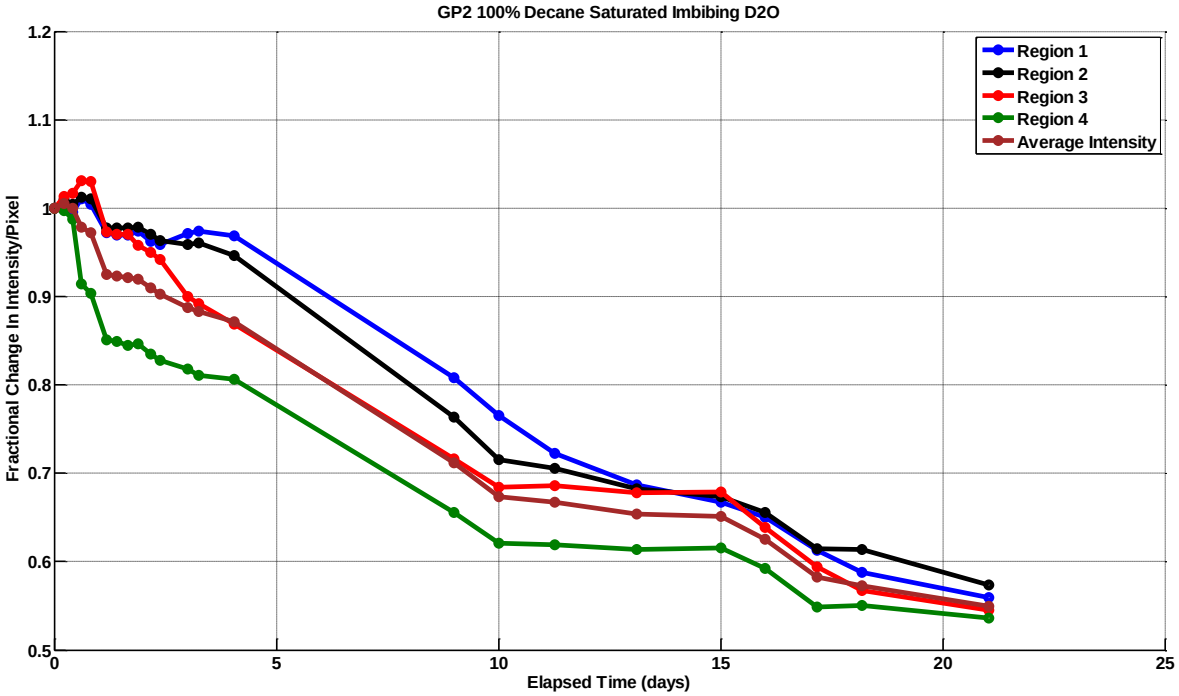

Figure 10: The relative change in average intensity per pixel vs elapsed time for each of the four regions of interest (Figure 6) is shown. As expected, the average intensity per pixel drops over time for each region of interest. This is because D_2O is imbibing into the rock and displacing the decane. In addition, the traces show that the average intensity per pixel changes slower the further from the imbibition front the region of interest is. However, by day twenty, the fractional change in intensity per pixel is almost the same for each region of interest. This indicates that the imbibition time is several weeks for tight samples.

Discussion

The change of saturation vs. time derived from the three-dimensional data for sample GP2 was consistent with the saturation vs time data derived from the T_2-distribution based wettability analysis done previously [Kelly S. et al., Kelly S. et al.]. It was also consistent with the saturation vs. time data derived from the D_2O data both previously [Kelly S. et al., Kelly S. et al.] and in this study. This gave us further confidence that our wettability analysis method is accurate and robust.

The three-dimensional data augmented the previous T_2-distribution based data in showing how imbibition spatially occurred within the sample. The three-dimensional imaging data showed that fluids do spontaneously imbibe completely and near-uniformly penetrate unconventional samples. However, the spontaneous imbibition can take weeks to reach steady state within the entire volume of the sample. This result has important consequences on the validity of our wettability analysis. As mentioned previously, our wettability analysis hinges on the assumption that the samples are uniformly saturated and that imbibition penetrates the entire rock. The results presented in this paper show that this assumption is not valid until sufficient imbibition time has elapsed; i.e., several weeks for tight samples. Before then the sample is not uniformly saturated and as a result the bulk T_2 distributions measured are not a true reflection of the pore size distribution across the entire sample. This makes using the bulk T_2 distributions measured during early times for the wettability analysis precarious. For example, the blue trace in the right panel of Figure 5 shows that the predicted brine saturation for sample GP2 oscillates between 20 and 40% until approximately day fifteen when the predicted saturation stabilizes and begins to agree well with the saturation measurements done with D_2O (Figure 5 – right panel – black and brown traces). This type of result was

seen in several of the samples we have investigated previously [Kelly S. et al., Kelly S. et al.] and is a direct consequence of the samples not being uniformly saturated until after at least fifteen days of imbibition. We now know that predicting wettability from this early bulk T_2-distribution data can lead to erroneous results. We have now modified our procedure to wait at least fifteen days before making a final determination of the wettability/saturation of a sample. In addition, the imbibition front should (if possible) be monitored with three-dimensional imaging to ensure that the sample is uniformly saturated prior to the final wettability analysis. Yet another option is to speed up the water uptake process by deploying a forced imbibition experimental setup. If three-dimensional imaging is employed, care should be taken to ensure that the sample is well sealed to eliminate H-D exchange leading to the creation of HDO in the bath surrounding the imbibing sample. The presence of HDO can interfere with the intensity of the observed image data leading to erroneous results.

Conclusions

This paper marks the conclusion of our work on adapting the NMR-based wettability index (NWI) methodology of Looyestijn et al. [Looyestijn, W. et al., Looyestijn, W. et al.] and applying it to unconventional rocks. In our previous work [Kelly S. et al., Kelly S. et al.] , we described a time-lapse imbibition data workflow for determining the steady state wettability of unconventional samples. Our method was applied to a variety of rock types and formations to test its robustness and learn about the wettability variation of major North America unconventional plays. We found that the NWI model implemented is well suited for data sets featuring complex oil and water T_2 spectra with multiple peaks. In addition, we have completed an extensive validation of our study employing D_2O measurements to confirm the oil/brine saturations predicted from the wettability analysis. In the current, paper we took this D_2O validation one step further and applied it to three-dimensional imaging. These three-dimensional D_2O images were employed to validate not only the observed oil and brine saturations but also that the imbibition front fully penetrates the core sample. Our wettability analysis hinges on the assumption that the samples are uniformly saturated and that imbibition penetrates the entire rock. The results presented in this paper show that this assumption is not valid until sufficient imbibition time has elapsed; i.e., several weeks for tight samples. Before then the sample is not uniformly saturated and as a result the bulk T_2 distributions measured are not a true reflection of the pore size distribution across the entire sample. This makes using the bulk T_2 distributions measured during early times for the wettability analysis precarious. Based on these results, we have now modified our procedure to wait at least fifteen days before making a final determination of the wettability/saturation of a sample. In addition, the imbibition front should (if possible) be monitored with three-dimensional imaging to ensure that the sample is uniformly saturated prior to the final wettability analysis.

We feel as though our method for determining the NMR-based wettability index (NWI) is robust and ready for more unconventional samples to be tested. We recommend expanding the three-dimensional analysis presented in this paper to include other UR rock types of varied textural complexity and heterogeneity, including laminated samples.

References

Kelly, S., Bonnie, R.J.M., Dick, M.J., Veselinovic, D., “NMR Wettability Index Measurements and Methods Compared on a Variety of Unconventional Samples.”, SPWLA Annual Symposium, Boston, MA, USA, 15-19 May 2021.

Looyestijn, W.J. and Hofman, J.P., “Wettability Index Determination by Nuclear Magnetic Resonance”, SPE 93624, presented at the MEOS, Bahrain, March 2005. Published in SPEREE April 2006, pp 146 – 153.

Looyestijn, W., Zhang, X., and Hebing, A., "How can NMR assess the wettability of a chalk reservoir", Society of Core Analysts, Vienna, Austria, 27 August-1 September 2017.

Kelly, S., Bonnie, R.J.M., Dick, M.J., Veselinovic, D., . “NMR Time-Lapse Wettability Assessments in Unconventional: Insights from Imbibition”, Unconventional Resources Technology Conference, Houston, TX, USA, 20-22 July 2020.

Geo-Spec 12-53 User Manual, Version 1.X, Oxford Instruments.

GIT Systems and LithoMetrix User Manual, Revision 1.9, Green Imaging Technologies.

Meiboom, S. and Gill, D., “Modified Spin-Echo Method for Measuring Nuclear Relaxation Times”, Review of Scientific Instruments (1958), 29, 688-691

Balcom, B.J., MacGregor, R.P., Beyea, S.D., Green, D.P., Armstrong, R.L. and Bremner, T.W. "Single Point Ramped Imaging with T_1 Enhancement (SPRITE)", Journal of Magnetic Resonance A (1996) 123, 131-134.